Title

RNA-antimicrobial peptide LL-37 complexes fuel a TLR- and NET-mediated inflammatory cycle of neutrophil activation in psoriasis

Running title

RNA and LL37 activate neutrophils in psoriasis

Authors

Franziska Herster[1], Zsofia Bittner[1], Sabine Dickhöfer[1], David Eisel[1,$], Tatjana Eigenbrod[2], Thomas Knorpp[3], Nicole Schneiderhan-Marra[3], Markus W. Löffler[1,4], Hubert Kalbacher[5], Dominik Hartl[6], Lukas Freund[7], Knut Schäkel[7], Martin Heister[8], Kamran Ghoreschi[8,9], Alexander N.R. Weber[1,*]

Affiliations

[1] Department of Immunology, University of Tübingen, Auf der Morgenstelle 15, 72076 Tübingen, Germany

[2] Department of Infectious Diseases, Medical Microbiology and Hygiene, University Hospital Heidelberg, Im Neuenheimer Feld 324, 69120 Heidelberg, Germany

[3] NMI Natural and Medical Sciences Institute at the University of Tübingen, Markwiesenstr. 55, 72770 Reutlingen, Germany

[4] Department of General, Visceral and Transplant Surgery, University Hospital Tübingen, Hoppe-Seyler-Str. 3, 72076 Tübingen, Germany

[5] Interfaculty Institute of Biochemistry, University of Tübingen, Hoppe-Seyler-Str. 4, 72076 Tübingen, Germany

[6] University Children's Hospital and Interdisciplinary Center for Infectious Diseases, University of Tübingen, Hoppe-Seyler-Str. 1, 72076 Tübingen, Germany

[7] Department of Dermatology, University Hospital Heidelberg, Im Neuenheimer Feld 440, 69120 Heidelberg, Germany

[8] Department of Dermatology, University Hospital Tübingen, Liebermeisterstr. 25, 72076 Tübingen, Germany

29 [9] Department of Dermatology, Charité – Universitätsmedizin Berlin, Charitéplatz 1, 10117 Berlin,
30 Germany

31

32 *** Contact information (Corresponding Author)**

33 Alexander N. R. Weber, Interfaculty Institute for Cell Biology, Department of Immunology, University
34 of Tübingen, Auf der Morgenstelle 15, 72076 Tübingen, Germany. Tel.: +49 7071 29 87623. Fax: +49
35 7071 29 4579. Email: alexander.weber@uni-tuebingen.de

36

37 **[$] Change of address/additional addresses**

38 David Eisel, GMP & T Cell Therapy Unit (G183), German Cancer Research Center, Im Neuenheimer
39 Feld 280, 69120 Heidelberg, Germany

40 Dominik Hartl, Galapagos Pharma, Basel, Switzerland

41 **Keywords**

42 Antimicrobial peptide LL-37, RNA, psoriasis, neutrophil, Toll-like receptor (TLR), neutrophil
43 extracellular trap (NET)

44 **Summary**

45 Human and bacterial RNA in complex with LL37 activates neutrophils via TLR8 to release cytokines,
46 chemokines and neutrophil extracellular traps (NETs). NETs and neutrophil-rich areas in psoriatic skin
47 contain RNA and LL37, suggesting RNA-LL37 may fuel a PMN-mediated and self-sustaining
48 inflammatory cycle in psoriasis.

49 **Abstract**

50 Psoriasis is an inflammatory autoimmune disease characterized by skin lesions showing strong
51 neutrophil (PMN) infiltration and high levels of the antimicrobial peptide, LL37, but the role of PMNs
52 in this context remains unclear. We here show that primary human PMNs, especially PMNs from
53 psoriasis patients, not only respond via TLR8 to human and bacterial RNA in complexed with LL37 by
54 cytokine-, chemokine- and neutrophil extracellular trap (NET)-release; they also actively release
55 additional RNA and LL37 in response to stimulation by the same complex and both RNA and LL37
56 were found to be highly abundant in psoriatic skin. Moreover, RNA-LL37-induced NETs propagated
57 PMN activation and could thus fuel a PMN-mediated and self-sustaining inflammatory loop that may
58 represent an unexpected early initiator or amplifying event in psoriasis. Given that TLR inhibitory
59 oligodeoxynucleotides prevented the cytokine production and NETosis of PMNs by RNA-LL37
60 complexes *in vitro*, our study also highlights TLR blockade as a potential therapeutic intervention
61 strategy in psoriasis.

62

63 ## Introduction

64 Psoriasis is an autoimmune disease of the skin with high incidence in Western countries (1.5-3%),
65 causing high socioeconomic and disease burden with limited but increasing treatment options
66 (Eberle et al., 2016; Griffiths and Barker, 2007). The most common form of psoriasis, plaque psoriasis,
67 is characterized by epidermal hyperplasia due to keratinocyte (KC) hyper-proliferation, increased
68 endothelial proliferation and an infiltrate of leukocytes, such as dendritic cells, T cells and,
69 prominently, polymorphonuclear neutrophils (PMNs)(Griffiths and Barker, 2007). The high and early
70 accumulation of PMNs in psoriatic plaques and micro-abscesses is well documented, as well as an
71 increase of PMNs in the circulation of psoriasis patients (Sen et al., 2013) (Schon et al., 2017).
72 However, it is unclear whether PMN infiltration represents a bystander phenomenon or has a causal
73 role in the development of the disease.

74 PMNs are known as a source of LL37, an amphipathic, positively-charged 37 amino acid peptide
75 generated from a precursor protein, the cathelicidin hCAP18, and highly abundant in psoriatic lesions
76 (Griffiths and Barker, 2007; Morizane and Gallo, 2012). LL37 is stored in the secondary granules of
77 PMNs, from which it can be released upon activation (Sorensen et al., 1997). Apart from acting as a
78 self-antigen for CD4 helper T cells in psoriasis patients (Lande et al., 2014), LL37 was previously
79 shown to form complexes with DNA or RNA that resisted nuclease degradation, were readily taken
80 up by plasmacytoid dendritic cells (pDCs), and triggered high Interferon (IFN) α and low Tumor
81 necrosis factor (TNF) or Interleukin (IL) 6 secretion from these cells (Ganguly et al., 2009; Lande et al.,
82 2007). Although type I IFNs contribute to psoriasis (Afshar et al., 2013; Yao et al., 2008), chemokines
83 and pro-inflammatory cytokines such as TNF, IL-1β or IL-23 are additionally required for immune cell
84 infiltration and T cell polarization, respectively (Ghoreschi et al., 2007). Since pDCs are comparatively
85 low producers of these psoriasis-initiating inflammatory cytokines and do not accumulate to high
86 numbers in psoriatic skin, this raises the question whether nucleic acid-LL37 sensing by other
87 immune cells, particularly PMNs, may contribute more prominently to initial inflammatory
88 cytokine/chemokine milieu observed in psoriasis.

89 In contrast to pDCs, PMNs are known producers of considerable amounts of various cytokines and
90 chemokines (Kruger et al., 2015; Tecchio et al., 2014; Terui et al., 2000). Additionally, PMNs are able
91 to undergo neutrophil extracellular trap (NET) formation (NETosis), an activation-induced process
92 leading to the extrusion of nuclear DNA (Brinkmann et al., 2004), as well as cellular proteins,
93 including LL37 (Radic and Marion, 2013). Like pDCs, PMNs express multiple pattern recognition
94 receptors (PRRs) of the Toll-like receptor (TLR) family, namely TLR2, 4, 8 (Berger et al., 2012) and 9
95 (Lindau et al., 2013), but not TLR3 or TLR7 (Berger et al., 2012). TLRs directly bind activating ligands,
96 typically so-called microbe-associated molecular patterns (MAMPs) absent from the host (Kawasaki

97 and Kawai, 2014); however, when they can gain access to endosomal compartments - for example by
98 complex formation with LL37 - host nucleic acids are able to trigger the endosomal TLRs 3, 7, 8
99 (sensing double-stranded or single-stranded RNA, respectively) or TLR9 (sensing DNA). TLR7
100 expression in humans is restricted to pDC and (only inducibly) to B cells. TLR8 thus appears to be the
101 primary receptor for foreign (and potentially host-derived) single-stranded RNA in humans
102 (Eigenbrod et al., 2015).

103 PMNs theoretically combine the abilities (i) to release LL37 and nucleic acids as components of
104 immuno-stimulatory ligands via NETosis; (ii) to potentially sense such ligands via TLRs; and (iii) to
105 secrete chemo-/cytokines. These mechanisms were never shown to act in concert but we speculated
106 whether LL37-mediated DNA or RNA sensing via TLRs in PMNs might initiate and fuel inflammatory
107 chemo-/cytokine production and thus inflammation and immune cell infiltration in psoriatic skin. We
108 here present experimental evidence that human primary PMNs readily respond to RNA-LL37
109 complexes, but not RNA alone, leading to the release of a broad array of chemokines and cytokines à
110 and can be therapeutically blocked by inhibitory oligodeoxynucleotides (iODNs). Unexpectedly, RNA-
111 LL37 also triggered the release of NETs, which contained additional LL37, RNA and DNA and could
112 activate further PMN, thereby providing the basis for a self-propagating inflammatory cycle.

113 ## Results

114 **LL37 promotes RNA uptake and induces TLR8-mediated PMN activation**

115 Previous results indicated that human primary PMNs can respond to RNA and DNA when stimulated
116 for >12 h, albeit at much lower levels than when stimulated with the nucleoside analog TLR7/8
117 agonist, R848 (Janke et al., 2009; Lindau et al., 2013). We sought to re-evaluate these findings using
118 highly purified primary PMNs assayed within a short time period (4 h) that excludes secondary
119 release effects, e.g. by apoptosis (Fig. S1A). The TLR7/8 agonist R848, like the TLR4 agonist, LPS,
120 elicited robust IL-8 release but only LPS triggered CD62L shedding; phospho-thioate (PTO) synthetic
121 CpG ODN, a typical TLR9 agonist, also strongly activated IL-8 release and CD62L shedding (Fig. 1A,
122 Table S1). However, unmodified, natural phospho-diester DNA ODN or human genomic DNA elicited
123 neither IL-8 release nor CD62L shedding, irrespective of whether they were complexed with LL37 (Fig.
124 1B). In contrast, in pDC LL37 binding of natural DNA triggered potent TLR9 responses (Lande et al.,
125 2007). In the absence of LL37, single-stranded synthetic RNA40 (henceforward referred to as 'RNA')
126 barely caused IL-8 release when applied at equimolar concentrations with R848 (Fig. 1C). This
127 suggests that on their own neither RNA nor DNA are able to trigger primary PMN responses. This
128 may be due to the endosomal localization of TLR8 and 9, which R848 and CpG can apparently access,
129 whereas RNA and normal DNA cannot (Kuznik et al., 2011). However, robust IL-8 release and
130 moderate CD62L shedding were observed when RNA was complexed with LL37 (Fig. 1C and *cf.* Fig.
131 2E). To check whether PMNs could engage RNA-LL37 complexes, live PMNs were seeded and RNA-
132 LL37 complexes added for 20 min before fixing the cells for electron microscopy analysis. As shown in
133 Fig. 1D, PMNs were found in proximity to fiber-like structures corresponding to RNA-LL37 complexes
134 (Schmidt et al., 2015). Flow cytometry using AlexaFluor (AF) 647-labeled RNA showed that LL37 also
135 promoted the uptake of complexed RNA: >20% of PMNs incubated with labeled RNA in the presence
136 of LL37 were AF647-positive within 60 min, compared to 5% in the absence of LL37 (Fig. 1E).
137 ImageStream bright-field cytometry confirmed that this was not due to external/surface binding of
138 labeled RNA but rather internalization (Fig. 1F, G). Bright-field fluorescence microscopy with Atto488-
139 labeled LL37 showed co-localization of AF647-RNA and Atto488-LL37 in intracellular compartments
140 (Fig. 1H) where endosomal TLRs are expressed (Berger et al., 2012). To pharmacologically explore
141 whether an endosomal TLR might be involved, we investigated the effect of chloroquine, a well-
142 known inhibitor of endosomal TLRs that was non-toxic for PMNs (Fig. S1B). Indeed IL-8 release from
143 primary PMNs in response to RNA-LL37 and CpG ODN (positive control) was significantly reduced by
144 chloroquine addition (Fig. 1I and S1C, respectively). As chloroquine does not affect cytoplasmic RNA
145 sensors (e.g. RIG-I) (Matsukura et al., 2007), this implicates an endosomal TLR in RNA-sensing. We
146 next sought to check whether the observed effect on cytokine release extended to normal RNA from

147 mammalian cells which may be more physiologically relevant in the context of psoriasis. As shown in
148 Fig. 1J, human mRNA significantly induced IL-8 release, but only in combination with LL37. Since
149 microbiome analyses have recently revealed alterations in staphylo- and streptococcal skin
150 colonization in psoriasis patients (Alekseyenko et al., 2013) and bacterial RNA is an emerging
151 immuno-stimulatory pattern (Eigenbrod and Dalpke, 2015), we also tested whether LL37 promoted *S.*
152 *aureus*, i.e. bacterial RNA (bRNA) activation of PMNs. Fig. 1K shows that bRNA significantly
153 stimulated IL-8 release similarly to RNA40 when complexed with LL37. Taken together this suggests
154 that uptake of RNA is promoted by LL37 and directs RNA to intracellular compartments from which
155 TLR sensing and activation leading to cytokine release can occur – both in response to mammalian
156 and bacterial/foreign RNA.

157 **RNA-LL37 complexes prompt release of multiple pro-inflammatory cytokines and chemokines,**
158 **especially in psoriasis PMNs.**

159 To test whether RNA-LL37 also promoted the release of cytokines other than IL-8, we screened
160 supernatants of stimulated PMNs by Luminex multiplex analysis and detected TNF, IL-1β, IL-6, and –
161 unexpectedly – IL-16 and MIP-1β primarily or exclusively in RNA-LL37-stimulated cell supernatants,
162 respectively (Fig. S2A,B). Despite variation between donors, this was confirmed by cytometric bead
163 arrays analyses (Fig. 2A-C) and ELISA (Fig. 2D, E) in samples from more donors. To our knowledge,
164 active receptor-mediated release of the chemoattractants, IL-16 (also known as Lymphocyte
165 Chemoattractant Factor, LCF) and MIP-1β (also known as Chemokine (C-C motif) Ligand, CCL4) from
166 primary human PMNs has so far not been reported. In fact, release of IL-16 was also boosted by LL37
167 alone (Fig. 2D) and MIP-1β was strongly released from PMNs in response to RNA-LL37 complexes but
168 not RNA alone (Fig. 2E).

169 Since IL-16 and MIP-1β are known chemoattractants for CD4 T cells and a variety of other immune
170 cells (Cruikshank and Little, 2008; Menten et al., 2002; Roth et al., 2016), we checked whether IL-16
171 or MIP-1β, at the concentrations observed in this study, could influence the migration and infiltration
172 of additional immune cells, which is a hallmark of psoriatic plaques (Schon et al., 2017). Transwell
173 experiments with peripheral blood mononuclear cells (PBMCs) from healthy human donors (upper
174 well) and IL-16 (300 and 1500 pg/ml), MIP-1β (30 and 150 pg/ml) or SDF-1α as a control (lower well,
175 Fig. S2C-E) showed that the lowest concentration of both cytokines induced a donor-dependent
176 increase in the number of CD3+CD4+ helper, CD3+CD8+ cytotoxic T cells as well as CD14+HLA-DR+
177 monocytes (Figs. 2F-H). Possibly due to a non-linear dose response relationship observed for some
178 cytokines (Atanasova and Whitty, 2012), higher concentrations had a weaker effect in some donors.
179 Owing to the donor-to-donor variation generally observed throughout in the human system, only a
180 non-significant, moderate effect was observed. We separately tested whether RNA or RNA-LL37 in
181 the lower chamber had any direct influence on the migration of these cell populations and noted an

182 unexpected and significant chemoattractive effect on $CD4^+$ T cells, in response to RNA-LL37 (Fig. 2I).
183 Interestingly, the presence of PMNs, regardless of stimulus, was sufficient to attract a variety of
184 other cells (results not shown) due to a so far unknown mechanism.

185 When repeating the above described stimulation experiments with psoriasis PMNs compared to
186 PMNs from healthy donor, both release of both IL-8 and MIP-1β was significantly increased two-fold
187 in response to RNA-LL37 (Fig. 2J, K), but not to LPS (Fig. S2F, G). Whereas IL-8 release in response to
188 'RNA alone' (i.e. without LL37) was indistinguishable from 'unstimulated' samples in healthy donor
189 PMNs (*cf.* also Fig. 1C), psoriasis PMNs treated with 'RNA alone' (Fig. 2J, arrow) produced significantly
190 more IL-8 than both 'unstimulated' psoriasis PMNs and healthy donor PMNs stimulated with 'RNA
191 alone') Since in healthy donors, RNA seemed to strongly depend on LL37 for efficient PMN uptake
192 and stimulation (*cf.* Fig. 1E, F) and PMNs are the major contributors to elevated LL37 in psoriasis, we
193 speculated whether psoriasis PMNs might constitutively secrete LL37 and this endogenous LL37
194 might promote an increased responsiveness to exogenously added RNA alone in psoriasis PMNs.
195 Psoriasis PMNs constitutively showed an increased baseline release of LL37 compared to healthy
196 donors (Fig. 2L). We conclude that the combination of RNA with LL37 triggers the release of an
197 extended array of pro-inflammatory cytokines and effective chemoattractants not triggered by RNA
198 alone. This was more prominent in psoriasis PMNs, potentially due to a higher abundance of PMN-
199 derived LL37.

200 **RNA-LL37 complexes trigger the release of RNA- and LL37-containing NETs**

201 Our data so far indicate that RNA and LL37 might contribute to cytokine-mediated inflammation and
202 immune infiltration in neutrophil-containing skin lesions in psoriasis patients. Such neutrophil
203 responses would probably be temporary, unless RNA-LL37 triggered the release of additional RNA
204 and LL37. PMN NETs are known to contain extracellular DNA that acts as an immune stimulant of
205 pDCs when complexed with LL37 (Lande et al., 2011). But DNA-LL37 cannot activate PMNs (*cf.* Fig.
206 1B) and RNA release by NETosis has not been shown. NETs would thus only propagate PMN
207 activation in case they also contained RNA. We therefore next tested (i) whether RNA-LL37 induces
208 NETosis and (ii) whether NETs contain RNA. Interestingly, electron microscopy (Fig. 3A) and a
209 neutrophil elastase-based NET assay (see Methods) confirmed significant neutrophil elastase release,
210 a hallmark of NETosis, in response to RNA-LL37 and PMA (positive control), but also with LL37 alone
211 (Fig. 3B). However, fluorescence microscopy analysis of fixed PMN samples established that only
212 RNA-LL37 complexes, and not LL37 alone, prompted the formation of LL37-positive NET-like
213 structures (Fig. 3C). To check whether the NETs also contained RNA, an RNA-selective fluorescent
214 dye, SYTO RNAselect, was used to stain NETs. This staining showed released endogenous RNA (green)
215 in both PMA and RNA-LL37-mediated NETs (Fig. 3C). Although the dye's specificity for RNA has been
216 established already (Li et al., 2006) we confirmed that RNA staining, but not DNA staining, was

217 sensitive to RNase A and thus RNA-specific (Fig. S3A, B). The presence of cellular RNA in NET
218 structures was also confirmed by the use of specific Abs against pseudo-uridine (ΨU), a nucleotide
219 absent from both DNA and also the synthetic RNA40 used for LL37 complex formation and
220 stimulation (Figs. 3D). Furthermore, using AF647-labeled or AF488-labeled synthetic RNA for in vitro
221 stimulation both the extracellular SYTO RNAselect and anti-ΨU signals could be unequivocally
222 attributed to de-novo released 'cellular RNA' and distinguished from exogenously added 'stimulant
223 (synthetic) RNA' by (Fig. S3C, D). The same applied to LL37, using Atto488-LL37 (Fig. S3E). To further
224 exclude artefacts that might arise from staining fixed samples, RNA-LL37 mediated NETosis was also
225 analyzed and confirmed using live-cell time-lapse analysis of PMNs (Fig. 3E and Movies S1-S3,
226 quantified in Fig. 3F). Interestingly, in PMNs captured on the verge of NETosis, RNA staining in a
227 granula-like fashion could be clearly observed (Fig. S3F). Thus, RNA-LL37 activates primary PMNs to
228 release NETs. In addition to the well established NET components DNA and LL37, these NETs contain
229 further RNA as a so far unappreciated component.

230 Increased levels of NETs containing DNA have already been reported in the blood and skin of
231 psoriasis patients (Hu et al., 2016). To check whether this was also the case for RNA, we stained skin
232 sections with SYTO RNAselect, anti-LL37 and anti-NE Abs. As expected, psoriatic skin was highly
233 positive for LL37; interestingly, the RNA signal was also generally stronger when compared to healthy
234 skin, using identical staining and microscopy settings (Fig. 3G). RNA and LL37 were frequently co-
235 localized in samples with high PMN infiltration (anti-NE staining), (Fig. 3H and Movie S4). This was
236 SYTO RNAselect specificity was confirmed using anti-Ψ staining on skin sections (Fig. S3G). This
237 indicates that RNA-LL37 complexes may act as physiologically relevant activators in psoriatic skin.

238 However, if RNA-LL37 complexes truly triggered a NET-mediated self-propagating inflammatory loop
239 of repetitive PMN activation, we would expect that isolated NET content would act in a manner
240 similar to RNA-LL37 and activate naïve PMNs to NETose. Indeed, when we harvested NETs from
241 PMNs stimulated either with PMA, RNA-LL37 complexes, LL37 or left untreated (mock),and
242 transferred them to unstimulated naïve PMNs, these responded with de-novo NET release in turn,
243 monitored by fixed microscopy of stimulated PMNs (Fig. 3J, quantified in I).. Collectively, RNA-LL37
244 complexes were found in psoriatic skin and in vitro prompted the release of NETosis. These NETs in
245 turn had the capacity to activate naive PMNs, thus providing the requirements for a self-propagating
246 feed forward loop of immune activation that might apply to skin PMNs.

247 **RNA-LL37 complexes and NETs activate PMNs via TLR8/TLR13**

248 In order to gain an insight which receptor mediates the observed effects of RNA-LL37 in primary
249 PMNs, we first compared BM-PMNs from WT mice and mice deficient for *Unc93b1*, a critical
250 chaperone of endosomal TLRs (Eigenbrod et al., 2012). Evidently, not only the cytokine response of

251 BM-PMNs to bRNA+LL37 (and the control stimulus R848) was strictly dependent on *Unc93b1* and
252 thus endosomal TLRs (Fig. 4A); NETosis triggered by bRNA-LL37 complexes, but not the TLR-
253 independent control stimulus PMA, was also *Unc93b1* dependent (Fig. 4B). Given that RNA is a
254 known dual TLR7 and TLR8 agonist (Colak et al., 2014) and primary human PMNs do not express *TLR7*
255 (Berger et al., 2012), we suspected TLR8 to mediate RNA-LL37-mediated PMN activation.
256 Unfortunately, human primary PMNs are not amenable to RNAi or genetic editing. Therefore, we first
257 tested the responsiveness of BM-PMNs from mice deficient for TLR13, the functional counterpart of
258 human TLR8 and primary bRNA sensor in mice (Eigenbrod and Dalpke, 2015). In murine PMNs both
259 cytokine and NET responses to bRNA+LL37 were strictly dependent on TLR13 (Fig. 4A, C), whereas
260 the negative controls LPS, *E. c*oli or PMA were not, respectively (*cf.* Fig. 4A or B, respectively).
261 Complementarily, the failure of *TLR8* CRISPR-deleted BlaER1 monocytes (Vierbuchen et al., 2017) to
262 respond to RNA-LL37 complexes and a novel TLR8-specific small molecule, TL8, (Fig. 4D) indicated a
263 dependence of RNA-LL37 immunostimulatory activity on TLR8 in the human cells, including PMNs.
264 Thus the stimulatory potential of RNA-LL37 complexes can be considered to be dependent on
265 TLR8/TLR13 as a NET-triggering sensing system.

266 **PMN cytokine release and NET formation by RNA-LL37 can be blocked by iODNs**

267 Having identified TLR8 as the responsible receptor in humans, we next wondered whether PMN
268 activation by RNA-LL37 could be blocked at the level of TLR activation by so-called inhibitory
269 oligonucleotides (iODNs). IRS869, IRS661 and IRS954 represent such TLR7 and 9-inhibitory iODNs that
270 were recently proposed for the treatment of another autoimmune disease, namely systemic lupus
271 erythematosus (SLE), whereas IRS546 was used as a non- 'control' ODN inhibitory (Barrat and
272 Coffman, 2008; Barrat et al., 2005; Duramad et al., 2005; Guiducci et al., 2010). Given the similarities
273 between endosomal TLRs (Colak et al., 2014), we speculated that some of these iODNs could
274 potentially also block TLR8, but the effects of iODNs on this receptor have not been studied
275 systematically. HEK293T cells do not express TLR7-9 but can be rendered responsive to their agonists
276 by exogenously expressing TLR7, TLR8 or TLR9 (control) upon transfection (Colak et al., 2014). In
277 HEK293T cells transfected and stimulated in this way, IRS869 and IRS954 blocked NF-κB activation in
278 response to R848 for TLR7 and 8 (Figs. S4A and B) and CpG for TLR9 (Fig. S4C). IRS661 effectively
279 blocked TLR7- but not TLR9-mediated activation. Paradoxically, IRS661 strongly increased R848-
280 mediated NF-κB activation via TLR8 (Fig. S4B), similar to observations made for T-rich ODNs
281 combined with R848 (Jurk et al., 2006) and highlighting the differences between R848 and RNA
282 reported previously (Colak et al., 2014). However, for RNA complexed with DOTAP (a synthetic
283 complexing agent promoting endosomal uptake (Yasuda et al., 2005), similarly to LL37), all three
284 iODNs blocked TLR8-mediated NF-κB activation (Fig. 4E). As the 'control' ODN IRS546 blocked NF-κB
285 activation in response to TLR7-9 stimulation, in our hands it did not represent a proper control unlike

286 previously published (Barrat et al., 2005). Nevertheless, the effects seemed specific for endosomal
287 TLR signaling as the effect of all iODNs on NF-κB activity induced by TNF (a non-TLR receptor pathway
288 activating NF-κB, Fig. S4D) or MyD88 overexpression (TLR receptor-independent NF-κB activation,
289 Fig. S4E) were minor. Having excluded a toxic effect on primary PMNs (Fig. S4F), we investigated
290 whether the observed effects could be transferred to endogenous TLR8 activation in primary PMNs,
291 where LL37 as a physiologically relevant uptake reagent was again used. Here, we found that iODNs
292 IRS661 and IRS954 were able to inhibit IL-8 release by primary PMNs from healthy donors in
293 response to RNA-LL37 at nanomolar iODN concentrations (Fig. 4F), whereas LPS-mediated IL-8
294 release was unaffected (Fig. S4G and (Saitoh et al., 2012)). The blocking effect extended to MIP-1β
295 (Fig. 4G), similar to the effect observed for chloroquine (Fig. S4H). Importantly, RNA-LL37-elicited
296 NETosis by primary human PMNs could be effectively blocked by nanomolar concentrations of
297 IRS661 (Fig. 4H, quantified in Fig. 4I). These results are in agreement with the observed TLR8-
298 dependence and iODN-mediated inhibition of NETosis in HIV infections (Saitoh et al., 2012) and
299 indicate an applicability to RNA-LL37 complexes. In conclusion, known pre-clinical iODNs are able to
300 block RNA-LL37-mediated cytokine and NET release.

301 **Discussion**

302 Although systemic therapies with biologicals have brought benefit for many psoriasis patients in
303 industrialized countries (Eberle et al., 2016), psoriasis remains a significant health problem
304 worldwide. One reason is that triggers and mechanisms leading to disease chronification,
305 exacerbation and flare-ups are not well understood. This uncertainty also applies to the role of PMNs
306 in these processes (Schon et al., 2017). Since PMNs can release nucleic acids, constitute the main
307 sources of LL37 in humans and congregate in psoriatic skin, we chose to study PMN RNA-LL37-
308 mediated responses after identifying TLR8 as an RNA receptor on PMNs (Berger et al., 2012). We
309 now provide novel evidence that RNA-LL37 can directly and TLR8-dependently activate PMNs to
310 release chemo-/cytokines and NETs, and that RNA originated from NETs could serve as a novel
311 immunostimulatory component within NETs, which has not been appreciated so far. Interestingly,
312 insect NETs contain primarily RNA rather than DNA (Altincicek et al., 2008), and eosinophils pre-store
313 RNA within their granules (Behzad et al., 2010). RNA may thus be a common and functionally
314 important NET component that has not been described for mammalian immune cells and ought to be
315 explored further. Given that RNA can also amplify responses to other PRR ligands (Noll et al., 2017),
316 the role of RNA will thus be interesting to study in other NET-related disease, e.g. SLE (Gestermann et
317 al., 2018), atherosclerosis (Warnatsch et al., 2015) and even cancer (Gregoire et al., 2015), where the
318 focus so far has been largely on DNA.

319 Recently, the effects of DNA-/RNA-LL37 complexes on pDCs were reported as a novel mechanism in
320 psoriasis inflammation (Ganguly et al., 2009; Lande et al., 2007). However, since pDC are only a
321 minor cell population even in psoriatic skin and they cannot release nucleic acids, their contribution
322 to cell-mediated inflammation and the provision of self-ligands is restricted to amplifying an already
323 ongoing pathology, first requiring pDC-attracting chemokines and an existing presence of self-ligands
324 in the skin. We found that the combination of RNA and LL37 produces an inflammatory ligand that is
325 not only directly sensed by PMNs; it also prompted the release of further components for additional
326 RNA-LL37 and DNA-LL37 complexes from PMNs. Whereas for pDCs both "inflammatory ingredients",
327 RNA or DNA and LL37, will need to be provided by another cellular source first, a small number of
328 activated and NETing PMNs – by releasing both, LL37 and RNA/DNA – may spark potent, self-
329 propagating inflammation *inter pares* and *in situ.* Following an initial activation of PMNs by
330 endogenous RNA from damaged skin cells (so-called Köbner phenomenon) or by bacterial
331 infection/RNA (Eigenbrod and Dalpke, 2015 and manuscript in press[1];*cf.* Fig. 1K) immune activation
332 may get out of control due to chemokine release and NET formation (and thus nucleic acid and LL37

[1] Anna Hafner, Ulrike Kolbe, Isabel Freund, Virginia Castiglia, Pavel Kovarik, Tanja Poth, Franziska Herster, Markus A. Weigand, Alexander N. Weber, Alexander H. Dalpke and Tatjana Eigenbrod: Crucial role of nucleic acid sensing via endosomal Toll-like receptors for the defense of *Streptococcus pyogenes in vitro* and *in vivo*; Front. Immunol. | doi: 10.3389/fimmu.2019.00198.

333 extrusion (Neumann et al., 2014)) which has been observed in the skin of psoriasis patients (Hu et al.,
334 2016). Although the concentration of the cytokines released after 4 h stimulation was moderate,
335 release over longer time periods and the sheer number of PMNs found in psoriatic skin may
336 nevertheless contribute substantially to local inflammation and attraction of additional leukocytes
337 over time. The PMN-mediated ongoing release of NET DNA, RNA and LL37 would eventually enable
338 pDCs and other immune cells to join the vicious cycle of activation fueled by endogenous nucleic
339 acids (Fig. S5) (Chamilos et al., 2012; Ganguly et al., 2009; Lande et al., 2007). Additionally, cytokine-
340 mediated inflammation is known to favor KC hyper-proliferation (Hanel et al., 2013), LL37 production
341 (Schauber et al., 2007), TLR9 responsiveness (Morizane et al., 2012) and IFN production (Zhang et al.,
342 2016), as well as T cell and monocyte attraction and polarization (Ghoreschi et al., 2007). In
343 conclusion, our study provides a plausible explanation how PMNs may contribute to early disease
344 development and, based on the observed effects of iODNs on PMN activation, warrants the further
345 exploration of TLR pathways and PMNs as targets for restricting innate immune activation in psoriatic
346 skin.

347 Materials and Methods

348 **Reagents**

349 All chemicals were from Sigma unless otherwise stated. PRR agonists and LL37 were from Invivogen
350 except RNA40 (iba Lifescience, normal and AF647- or AF488-labeled) and CpG PTO 2006 (TIB
351 Molbiol), see Table S2 and 3. iODNs used in this study with their respective sequences are listed in
352 Table S3 and were from TIB Molbiol. Total human mRNA was isolated from HEK293T cells using the
353 RNeasy kit on a QIAcube, both from QIAGEN. *S. aureus* RNA was isolated as described (Eigenbrod et
354 al., 2015). Genomic human DNA was isolated from whole blood using QIAamp DNA Blood Mini Kit
355 from Qiagen (51106) and phosphodiester DNA from TIB Molbiol. LL37 was from InvivoGen (see Table
356 S2) and DOTAP from Roth, L787.2. LL37 was Atto488 (from Atto-Tec as a carboxy-reactive reagent)-
357 labeled using standard procedures. For complex formation 5.8 µM RNA40 (approximately 34.4 µg/ml
358 and equimolar to R848 used in this setting), 1 µM ssDNA (approximately 20 µg/ml and equimolar to
359 CpG used in this setting, sequence see Table S3), genomic DNA (20 µg/ml) or bacterial RNA (10
360 µg/ml) was mixed together with 10 µg LL37 (see Table S2, Atto-488 where indicated) and left for one
361 hour at RT. For experiments with BM-PMNs, 1.25 µg bacterial RNA was complexed with 2.5 µg LL37.
362 For the RNA-only or LL37-only conditions, the same amounts and volumes were used replacing one
363 of the constituents by sterile, endotoxin-free H_2O. Ficoll was from Millipore. Antibodies used for flow
364 cytometry, ImageStream analysis or fluorescence microscopy are listed in Table S4 as well as the
365 recombinant cytokines used in this study. Constructs used for HEK293T transfection are listed in
366 Table S5.

367 **Study participants and sample acquisition**

368 All patients and healthy blood donors included in this study provided their written informed consent
369 before study participation. Approval for use of their biomaterials was obtained by the local ethics
370 committees at the University Hospitals of Tübingen and Heidelberg, in accordance with the principles
371 laid down in the Declaration of Helsinki as well as applicable laws and regulations. All blood or skin
372 samples obtained from psoriasis patients (median age 41.8 years, PASI >10, no systemic treatments
373 at the time of blood/skin sampling) were obtained at the University Hospitals Tübingen or
374 Heidelberg, Departments of Dermatology, respectively, and were processed simultaneously with
375 samples from at least one healthy donor matched for age and sex (recruited at the University of
376 Tübingen, Department of Immunology). Skin sections were from 12 patients with Plaque Psoriasis
377 and 1 patient with Psoriasis guttata.

378 **Mice and isolation of bone-marrow derived PMNs (BM-PMNs)**

379 *Unc93b1*$^{3d/3d}$-(Tabeta et al., 2006), *Tlr13*-deficient (Li and Chen, 2012) mice (both C57BL/6
380 background) and WT C57BL/6 mice between 8 and 20 weeks of age were used in accordance with
381 local institutional guidelines on animal experiments and under specific locally approved protocols for
382 sacrificing and *in vivo* work. All mouse colonies were maintained in line with local regulatory
383 guidelines and hygiene monitoring. Bone-marrow (BM)-PMNs were isolated from the bone marrow
384 using magnetic separation (mouse Neutrophil isolation kit, Miltenyi Biotec, 130-097-658) and
385 following the manufacturer's instructions. PMN stimulation was carried out for 5 hours at 37 °C and
386 5% CO_2. Thereafter supernatants were harvested and used for ELISA. For microscopy the cells were
387 stimulated for 16 h and subsequently stained.

388 **Neutrophil isolation and stimulation**

389 Whole blood (EDTA-anticoagulated) was diluted in PBS (Thermo Fisher, 14190-169), loaded on Ficoll
390 (1.077 g/ml, Biocoll, ab211650) and centrifuged for 25 min at 366 x g at 21 °C without brake. All
391 layers were discarded after density gradient separation except for the erythrocyte-granulocyte
392 pellet. Thereafter, erythrocyte lysis (using 1x ammonium chloride erythrocyte lysis buffer, see Table
393 S6) was performed twice (for 20 and 10 min) at 4 °C on a roller shaker. The remaining cell pellet was
394 carefully resuspended in culture medium (RPMI culture medium (Sigma Aldrich, R8758) + 10% FBS
395 (heat inactivated, sterile filtered, TH Geyer, 11682258)) and 1.6 x 10^6 cells/ml were seeded (24 well
396 plate, 96 well plate). After resting for 30 min at 37°C, 5% CO_2, the cells were pre-treated with
397 inhibitors (where indicated) for 30 min and subsequently stimulated with the indicated agonists for 4
398 hours (for ELISA) or for 30 min to 3 h (for FACS analysis or microscopy).

399 **PBMC isolation**

400 Whole blood (EDTA anticoagulant) was diluted in PBS. After density gradient separation using Ficoll
401 (described above), the PBMC layer was then carefully transferred into a new reaction tube and
402 diluted in PBS (1:1). The cell suspension was spun down at 1800 rpm for 8 min. The cells were then
403 washed twice more in PBS, resuspended in culture medium (RPMI + 10% FBS (heat inactivated) + 1%
404 L-glutamine), before counting and seeding.

405 **Generation and harvest of NETs**

406 Neutrophils were isolated as described above. $5x10^6$cells/ml were seeded per 10 cm dish, rested for
407 30 min and subsequently stimulated with RNA-LL37 complex, LL37 alone, PMA or left untreated
408 ('Mock' NETs) for 4 hours. Then the medium was removed and the cells were washed with PBS for
409 three times. Thereafter the adherent cell debris and generated NETs were scratched from the
410 surface, resuspended in culture medium and stored at -80°C before use.

411 **BlaER1 cells culture, transdifferentiation and stimulation**

412 BlaER1 cells (WT and $TLR8^{-/-}$, kindly provided and validated by Tim Vierbuchen and Holger Heine
413 from Borstel, Germany {Vierbuchen, 2017 #6405}) were cultured in VLE-RPMI (Merck Biochrom,
414 FG1415) + 10 % FBS, 1 % Pen/Strep (Gibco, 15140122), 1 % sodium pyruvate (100 mM, Gibco,
415 11360070), 1 % HEPES soluation (Sigma, H0887)). After reaching a cell concentration not higher than
416 2×10^6/ml the cells were seeded in a 6 well plates (1×10^6 cells per well) and transdifferentiated in
417 culture medium adding 150 nM β-estradiol, 10 ng/ml M-CSF and 10 ng/ml hIL-3 for 6 days including 2
418 medium changes (on day 2 and 5). On day 7 the adherent cells were counted again, seeded (96 well
419 plate, 5×10^4 cells per well) and left to rest for 1 h. Subsequently, they were stimulated for 18 h and
420 the supernatants were harvested and collected for ELISA measurements. The transdifferentiation
421 efficiency was verified by FACS analysis, using CD19, CD14 and CD11b as cell surface markers as
422 described {Rapino, 2013 #6445}.

423 **Flow cytometry**

424 After PMN isolation and stimulation, the purity and activation status of neutrophils was determined
425 by flow cytometry. 200 µl of the cell suspension was transferred into a 96 well plate (U-shape) and
426 spun down for 5 min at 322 x g, 4 °C. FcR block was performed using pooled human serum diluted
427 1:10 in FACS buffer (PBS, 1 mM EDTA, 2% FBS heat inactivated) for 15 min at 4 °C. After washing, the
428 samples were stained for approximately 20-30 min at 4°C in the dark. Thereafter, fixation buffer (4%
429 PFA in PBS) was added to the cell pellets for 10 min at RT in the dark. After an additional washing
430 step, the cell pellets were resuspended in 150 µl FACS buffer. Measurements were performed on a
431 FACS Canto II from BD Bioscience, Diva software. Analysis was performed using FlowJo V10 analysis
432 software.

433 **ELISA**

434 Cytokines were determined in half-area plates (Greiner, Bio-one) using duplicates or triplicates and
435 measuring with a standard plate reader. The assays were performed according to the manufacturer's
436 instructions (Biolegend, R&D systems), using appropriate dilutions of the supernatants. For LL37
437 determination a kit from HycultBiotech (HK321-02) was used following the manufacturer's
438 instructions.

439 **ImageStream analysis**

440 ImageStream analysis was used to analyze internalization of RNA-LL37 complexes using spot-counts
441 and tracking single cells. The cells were first seeded in a 96 well plate, 8 x 10^6 cells/ml, 125 µl per
442 well. Subsequently, they were stimulated for 1 hour with RNA-AF647 (IBA technologies) and/or LL37-
443 Atto488 (kindly provided by Hubert Kalbacher, University of Tübingen). FcR block and surface
444 staining (here CD15 PE) was performed as described above. After fixation, the cells were
445 permeabilized with 0.05 % Saponin (Applichem, A4518.0100) for 15 min at RT in the dark. After
446 washing, nuclei were stained with Hoechst 33342 (Sigma, B2261, 1 µg/ml) for 5 min at RT in the dark,
447 washed and resuspended in 50 µl FACS buffer and transferred into a 1.5 ml Eppendorf tube. At least
448 10.000 cells were acquired for each sample with 40x magnification using an ImageStream X MKII with
449 the INSPIRE instrument controller software (Merck-Millipore/Amnis). Data were analyzed with IDEAS
450 Image analysis software. All samples were gated on single cells in focus.

451 **Fluorescence Microscopy of fixed neutrophils**

452 The cells were seeded in a 96 well plate at 1.6 x 10^6 cells/ml, 125 µl per well. Subsequently they were
453 stimulated with the complexes for 30 min and 1 h using RNA-AF647/AF488 and/or LL37-Atto488. FcR
454 block, staining, fixation and permeabilization were performed as for Flow cytometry. The cell pellets
455 were resuspended in 50-100 µl FACS buffer. 40 µl of the cell suspension was pipetted on a Poly-L-
456 Lysine coated coverslip (Corning, 734-1005) and the cells were left to attach for one hour in the dark.
457 ProLong Diamond Antifade (Thermo Fisher, P36965) was used to mount the coverslips on uncoated
458 microscopy slides. For NET analysis PMNs were seeded in 24 well plates, containing Poly-L-Lysine
459 coated coverslips and stimulated with RNA-LL37 complexes or PMA (600 nM) for 3 hours. NETs were
460 fixed and stained using the protocol from Brinkmann et al.(Brinkmann et al., 2010). Where indicated,
461 100 µg/ml RNase A (DNase, protease-free, ThermoFisher, EN0531) was added after fixation and
462 incubated overnight at 37°C. RNA was stained using SYTO RNAselect Green fluorescent dye (Thermo
463 Fisher, 50 µM) or anti-ΨU antibody (see Table S4) and nuclear DNA was stained with Hoechst33342
464 (Thermo Fisher, 1 µg/ml). LL37 and PMNs were visualized using an unconjugated rabbit anti-LL37
465 antibody or unconjugated mouse anti-NE with subsequent staining with an AF647-conjugated anti-
466 rabbit or an AF594-conjugated anti-mouse antibody, respectively (see Supplementary Table S4), after

467 blocking with pooled human serum (1:10 in PBS). Secondary antibodies alone did not yield any
468 significant staining. The slides were left to dry overnight at RT in the dark and were then stored at 4
469 °C before microscopy. The measurements were conducted with a Nikon Ti2 eclipse (100x
470 magnification) and the analysis was performed using Fiji analysis software.

471 **Fluorescence Microscopy of tissue samples**

472 Skin samples from psoriasis patients with a PASI ≥ 10 and without systemic treatment, and healthy
473 skin samples paraffin-embedded according to standard procedures were deparaffinized and
474 rehydrated using Roti Histol (Roth, 6640.1) and decreasing concentrations of ethanol (100%, 95%,
475 80% and 70%). After rinsing in ddH_2O, antigen retrieval was performed by boiling for 10-20 min in
476 citrate buffer (0.1 M, pH=6). The skin tissue was then washed 3 times for 5 min with PBS. Blocking
477 was performed using pooled human serum (1:10 in PBS) for 30 min at RT. The primary antibody was
478 added either overnight at 4°C or for 1 hour at RT. After 3 washes, the secondary antibody was added
479 for 30 min at RT in the dark. After another 3 washes, SYTO RNAselect Green fluorescent dye (Thermo
480 Fisher, 50 µM) was added for 20 min at RT in the dark. Thereafter, the samples were washed again
481 and Hoechst 33342 (ThermoFisher, 1 µg/ml) was added for 5 min. Then 3 last washes were
482 performed before using ProLong Diamond Antifade (Thermo Fisher, P36965) for mounting. The
483 samples were left to dry overnight at RT in the dark before being used for microscopy or stored at
484 4°C. The specimens were analyzed on a Nikon Ti2 eclipse bright-field fluorescence microscope (10x-
485 60x magnification) and the analysis was performed using Fiji analysis software. Autofluorescence in
486 multiple channels typical for the stratum corneum was labeled "AF".

487 **Live cell imaging of primary neutrophils**

488 Human neutrophils were isolated by magnetic separation using MACSxpress whole blood neutrophil
489 isolation kit (Miltenyi Biotec, 130-104-434) and were seeded into a micro-insert 4 well dish (Ibidi
490 80406). Hoechst 33342 (1 µg/ml) and SYTO RNAselect Green fluorescent dye (50 µM) were added to
491 the cells and incubated for 20 min at 37°C, 5 % CO_2. Live cell imaging was performed by using Nikon
492 Ti2 eclipse bright-field fluorescence microscope (40x magnification) including a CO_2-O_2 controller
493 from Okolab. Measurements were started immediately after adding of stimuli. Time-lapse analysis
494 was performed by taking pictures every 3 min for at least 2 hours. Image analysis was performed
495 using NIS Elements from Nikon and Fiji analysis software.

496 **Luminex cytokine multiplex analysis**

497 All samples were stored at -70 °C until testing. The samples were thawn at room temperature,
498 vortexed, spun at 18,000 x g for 1 min to remove debris and the required sample volumes were
499 removed for multiplex analysis according to the manufacturer's recommendations. The samples
500 were successively incubated with the capture microspheres, a multiplexed cocktail of biotinylated,

501 reporter antibodies, and a streptavidin-phycoerythrin (PE) solution. Analysis was performed on a
502 Luminex 100/200 instrument and the resulting data were interpreted using proprietary data analysis
503 software (Myriad RBM). Analyte concentrations were determined using 4 and 5 parameter, weighted
504 and non-weighted curve fitting algorithms included in the data analysis package.

505 **Cytometric bead array**

506 A cytometric bead array was performed using the "Human inflammatory cytokine kit" from BD
507 Bioscience (551811) and following the manufacturer's instruction. 25 µl of samples and standards
508 were added to 25 µl of the capturing bead mixture. Additionally, 25 µl of PE detection reagent was
509 added to all tubes and incubated for 3 h at RT in the dark. Thereafter, 1 ml of wash buffer was added
510 to each tube and centrifuged at 200 x g for 5 minutes. The supernatant was carefully removed and
511 the pellet was resuspended in 300 µl wash buffer. Measurements were performed with the FACS
512 Canto II from BD Bioscience operated using Diva software. Analysis was performed with Soft Flow
513 FCAP Array v3 analysis software from BD Bioscience.

514 **Transwell experiments**

515 PBMCs and neutrophils were always used from the same donor in each experiment. Transwell inserts
516 were loaded with 100 µl of PBMC suspension (0.8 x 10^6 cells/insert). In the lower chamber, either
517 PMNs were seeded as described above (same plate size, same volume, same cell concentration)
518 using polycarbonate, 24 well plates, 3 µm pores, Corning, 734-1570) and stimulated for 4 h with
519 stimuli as indicated. Alternatively, media containing the stimuli only (i.e. no PMNs) or media
520 containing only MIP-1β (30 and 150 pg /ml), IL-16 (300 and 1500 pg/ml) or SDF-1α (control, 100
521 ng/ml) and no PMNs were added. After 4 h, the lower compartment was harvested and FACS staining
522 was performed as described above. The total number of migrated cells was acquired using counting
523 beads (Biolegend, 424902) on a FACS Canto II (BD Bioscience) with Diva software. Analysis was
524 performed using FlowJo V10 analysis software.

525 **Neutrophil elastase NETosis assay**

526 Neutrophil extracellular trap formation was determined using the colorimetric NETosis Assay Kit from
527 Cayman Chemicals based on the enzymatic activity of NET-associated neutrophil elastase. PMNs from
528 various healthy donors were isolated as described above and stimulated with RNA-LL37 complex, or
529 PMA and a calcium ionophore (A-23187) as positive controls for 1 or 3 hours. The assay was
530 performed following the manufacturer's instructions. The absorbance was then measured at 405 nm
531 using a standard plate reader.

532 **Transient transfection of HEK293T cells**

533 HEK293T cells were transiently transfected using the $CaPO_4$ method as described (Colak et al., 2014).
534 Cells were seeded in 24-well plates at a density of 14 x 10^5 cells/ml 2-3 h prior to transfection. For the
535 transfection of one well, 310 ng of plasmid DNA (100 ng TLR plasmid, 100 ng firefly luciferase NF-κB
536 reporter, 10 ng *Renilla* luciferase control reporter, and 100 ng EGFP plasmid) was mixed with 1.2 µl of
537 a 2 M $CaCl_2$ solution and filled up with sterile endotoxin-free H_20 to obtain a total reaction volume of
538 10 µl. After the addition of 10 µl of 2X HBS solution (50 mM HEPES (pH 7.05), 10 mM KCl, 12 mM
539 Glucose, 1.5 mM Na_2HPO_4), the mixture was then added to the cell suspension. As negative controls,
540 TLR coding plasmids were replaced by empty vectors carrying the appropriate backbone of the TLR
541 plasmids. After the addition of the transfection complexes, the cells were incubated either for 24 h
542 followed by stimulation, or kept for 48 h without stimulation (MyD88 expression). For stimulation,
543 the media was aspirated and replaced by fresh growth medium in which TNFα or the different TLR
544 ligands (R848, CpG, RNA40) with or without IRS were diluted to appropriate concentrations. TLR8
545 activation with RNA40 was facilitated by complexation of the RNA with DOTAP (L787.1, Roth). RNA40
546 and DOTAP were first diluted in 1X HBS separately. Next, RNA40/HBS was diluted 1:3 in DOTAP/HBS.
547 The solution was carefully mixed by pipetting up and down. After 15 min of incubation at RT, the
548 mixture was 1:6.7 diluted in growth medium (with or without IRS) and finally dispensed (500 µl/well)
549 into the wells containing transfected HEK293T cells. Each tested condition was measured in
550 triplicates. The cells were stimulated and inhibited for 24 h at 37°C.

551 **Dual Luciferase Reporter Assay**

552 After checking transfection efficiency via EGFP fluorescence microscopy, HEK293T supernatants were
553 aspirated and 60 µl of 1X passive lysis buffer (E194A, Promega) added per well. The plate was then
554 incubated for 15 min at RT on the plate shaker and subsequently stored at -80 °C for at least 15
555 minutes to facilitate complete cell lysis. After thawing, 60 µl were transferred into a V-bottom 96-
556 well plate and centrifuged for 10 min at 2500 rpm and 4 °C to pellet cell debris. 10 µl supernatant
557 were then transferred into a white microplate and each condition was measured in triplicates using
558 the FLUOstar OPTIMA device (BMG Labtech). Firefly and Renilla luciferase activity were determined
559 using the Promega Dual luciferase kit. Both enzyme activities were measured for 12.5 s with 24
560 intervals of 0.5 s, respectively. The data was analyzed by calculating the ratio of the two measured
561 signals, thereby normalizing each firefly luciferase signal to its corresponding Renilla luciferase signal.
562 The ratios were represented as the relative light units (RLU) of NF-κB activation.

563 **Statistics**

564 Experimental data was analyzed using Excel 2010 (Microsoft) and/or GraphPad Prism 6 or 7,
565 microscopy data with ImageJ/Fiji, flow cytometry data with FlowJo 10. In case of extreme values,

566 outliers were statistically identified using the ROUT method at high (0.5%) stringency. Normal
567 distribution in each group was always tested using the Shapiro-Wilk test first for the subsequent
568 choice of a parametric (ANOVA, Student's t-test) or non-parametric (e.g. Friedman, Mann-Whitney U
569 or Wilcoxon) test. p-values (α=0.05) were then calculated and multiple testing was corrected for in
570 Prism, as indicated in the figure legends. Values < 0.05 were generally considered statistically as
571 significant and denoted by * throughout. Comparisons made to unstimulated control, unless
572 indicated otherwise, denoted by brackets.

573 **Materials & Correspondence**

574 Please address requests to: Alexander N. R. Weber, Interfaculty Institute for Cell Biology, Department
575 of Immunology, University of Tübingen, Auf der Morgenstelle 15, 72076 Tübingen, Germany. Tel.:
576 +49 7071 29 87623. Fax: +49 7071 29 4579. Email: alexander.weber@uni-tuebingen.de

577 ## Supplementary Material

578 Is uploaded separately and includes 5 Supplementary figures and 6 supplementary tables.

579 ## Authorship contributions

580 F.H., Z.B., S.D., D.E., T.K. and N.S.M. performed experiments; F.H., Z.B., S.D., D.E., N.S.M. and
581 A.N.R.W. analyzed data; M.H., H. K., M.W.L., L.F., K.S., K.G. and T.E. were involved in sample and
582 reagent acquisition; F.H., D.H., K.G. and T.E. contributed to the conceptual development of the study;
583 F.H. and A.N.R.W. wrote the manuscript and all authors commented on an revised the manuscript;
584 A.N.R.W. coordinated and supervised the entire study. None of the authors declare competing
585 interests.

586 ## Acknowledgements

587 We thank S. Pöschel, J. Berger, S. Haen, K. Preissner, O. Sorensen and A. Dalpke for provision of
588 reagents, samples, technical support and/or helpful discussions and all healthy donors and patients
589 for participation in our study. This study was supported by the Deutsche Forschungsgemeinschaft
590 (German Research Foundation, DFG) CRC TR156 "The skin as an immune sensor and effector organ –
591 Orchestrating local and systemic immunity", the University of Tübingen and the University Hospital
592 Tübingen.

593 ## References

594 Afshar, M., A.D. Martinez, R.L. Gallo, and T.R. Hata. 2013. Induction and exacerbation of psoriasis
595 with Interferon-alpha therapy for hepatitis C: a review and analysis of 36 cases. J Eur Acad Dermatol
596 Venereol 27:771-778.

597 Alekseyenko, A.V., G.I. Perez-Perez, A. De Souza, B. Strober, Z. Gao, M. Bihan, K. Li, B.A. Methe, and
598 M.J. Blaser. 2013. Community differentiation of the cutaneous microbiota in psoriasis. Microbiome
599 1:31.

600 Altincicek, B., S. Stotzel, M. Wygrecka, K.T. Preissner, and A. Vilcinskas. 2008. Host-derived
601 extracellular nucleic acids enhance innate immune responses, induce coagulation, and prolong
602 survival upon infection in insects. J Immunol 181:2705-2712.

603 Atanasova, M., and A. Whitty. 2012. Understanding cytokine and growth factor receptor activation
604 mechanisms. Crit Rev Biochem Mol Biol 47:502-530.

605 Barrat, F.J., and R.L. Coffman. 2008. Development of TLR inhibitors for the treatment of autoimmune
606 diseases. Immunol Rev 223:271-283.

607 Barrat, F.J., T. Meeker, J. Gregorio, J.H. Chan, S. Uematsu, S. Akira, B. Chang, O. Duramad, and R.L.
608 Coffman. 2005. Nucleic acids of mammalian origin can act as endogenous ligands for Toll-like
609 receptors and may promote systemic lupus erythematosus. The Journal of experimental medicine
610 202:1131-1139.

611 Behzad, A.R., D.C. Walker, T. Abraham, J. McDonough, S. Mahmudi-Azer, F. Chu, F. Shaheen, J.C.
612 Hogg, and P.D. Pare. 2010. Localization of DNA and RNA in eosinophil secretory granules. Int Arch
613 Allergy Immunol 152:12-27.

614 Berger, M., C.Y. Hsieh, M. Bakele, V. Marcos, N. Rieber, M. Kormann, L. Mays, L. Hofer, O. Neth, L.
615 Vitkov, W.D. Krautgartner, D. von Schweinitz, R. Kappler, A. Hector, A. Weber, and D. Hartl. 2012.
616 Neutrophils express distinct RNA receptors in a non-canonical way. The Journal of biological
617 chemistry 287:19409-19417.

618 Brinkmann, V., B. Laube, U. Abu Abed, C. Goosmann, and A. Zychlinsky. 2010. Neutrophil
619 extracellular traps: how to generate and visualize them. J Vis Exp

620 Brinkmann, V., U. Reichard, C. Goosmann, B. Fauler, Y. Uhlemann, D.S. Weiss, Y. Weinrauch, and A.
621 Zychlinsky. 2004. Neutrophil extracellular traps kill bacteria. Science 303:1532-1535.

622 Chamilos, G., J. Gregorio, S. Meller, R. Lande, D.P. Kontoyiannis, R.L. Modlin, and M. Gilliet. 2012.
623 Cytosolic sensing of extracellular self-DNA transported into monocytes by the antimicrobial peptide
624 LL37. Blood 120:3699-3707.

625 Colak, E., A. Leslie, K. Zausmer, E. Khatamzas, A.V. Kubarenko, T. Pichulik, S.N. Klimosch, A. Mayer, O.
626 Siggs, A. Hector, R. Fischer, B. Klesser, A. Rautanen, M. Frank, A.V. Hill, B. Manoury, B. Beutler, D.
627 Hartl, A. Simmons, and A.N. Weber. 2014. RNA and imidazoquinolines are sensed by distinct TLR7/8
628 ectodomain sites resulting in functionally disparate signaling events. J Immunol 192:5963-5973.

629 Cruikshank, W., and F. Little. 2008. Interleukin-16: The Ins and Outs of Regulating T-Cell Activation.
630 Critical Reviews in Immunology 28:467-483.

631 Duramad, O., K.L. Fearon, B. Chang, J.H. Chan, J. Gregorio, R.L. Coffman, and F.J. Barrat. 2005.
632 Inhibitors of TLR-9 act on multiple cell subsets in mouse and man in vitro and prevent death in vivo
633 from systemic inflammation. J Immunol 174:5193-5200.

634 Eberle, F.C., J. Bruck, J. Holstein, K. Hirahara, and K. Ghoreschi. 2016. Recent advances in
635 understanding psoriasis. F1000Res 5:

636 Eigenbrod, T., and A.H. Dalpke. 2015. Bacterial RNA: An Underestimated Stimulus for Innate Immune
637 Responses. J Immunol 195:411-418.

638 Eigenbrod, T., L. Franchi, R. Munoz-Planillo, C.J. Kirschning, M.A. Freudenberg, G. Nunez, and A.
639 Dalpke. 2012. Bacterial RNA mediates activation of caspase-1 and IL-1beta release independently of
640 TLRs 3, 7, 9 and TRIF but is dependent on UNC93B. J Immunol 189:328-336.

641 Eigenbrod, T., K. Pelka, E. Latz, B. Kreikemeyer, and A.H. Dalpke. 2015. TLR8 Senses Bacterial RNA in
642 Human Monocytes and Plays a Nonredundant Role for Recognition of Streptococcus pyogenes. J
643 Immunol 195:1092-1099.

644 Ganguly, D., G. Chamilos, R. Lande, J. Gregorio, S. Meller, V. Facchinetti, B. Homey, F.J. Barrat, T. Zal,
645 and M. Gilliet. 2009. Self-RNA-antimicrobial peptide complexes activate human dendritic cells
646 through TLR7 and TLR8. The Journal of experimental medicine 206:1983-1994.

647 Gestermann, N., J. Di Domizio, R. Lande, O. Demaria, L. Frasca, L. Feldmeyer, J. Di Lucca, and M.
648 Gilliet. 2018. Netting Neutrophils Activate Autoreactive B Cells in Lupus. J Immunol 200:3364-3371.

649 Ghoreschi, K., C. Weigert, and M. Rocken. 2007. Immunopathogenesis and role of T cells in psoriasis.
650 Clin Dermatol 25:574-580.

651 Gregoire, M., F. Guilloton, C. Pangault, F. Mourcin, P. Sok, M. Latour, P. Ame-Thomas, E. Flecher, T.
652 Fest, and K. Tarte. 2015. Neutrophils trigger a NF-kappaB dependent polarization of tumor-
653 supportive stromal cells in germinal center B-cell lymphomas. Oncotarget 6:16471-16487.

654 Griffiths, C.E., and J.N. Barker. 2007. Pathogenesis and clinical features of psoriasis. Lancet 370:263-
655 271.

656 Guiducci, C., M. Gong, Z. Xu, M. Gill, D. Chaussabel, T. Meeker, J.H. Chan, T. Wright, M. Punaro, S.
657 Bolland, V. Soumelis, J. Banchereau, R.L. Coffman, V. Pascual, and F.J. Barrat. 2010. TLR recognition of
658 self nucleic acids hampers glucocorticoid activity in lupus. Nature 465:937-941.

659 Hanel, K.H., C. Cornelissen, B. Luscher, and J.M. Baron. 2013. Cytokines and the skin barrier. Int J Mol
660 Sci 14:6720-6745.

661 Hu, S.C., H.S. Yu, F.L. Yen, C.L. Lin, G.S. Chen, and C.C. Lan. 2016. Neutrophil extracellular trap
662 formation is increased in psoriasis and induces human beta-defensin-2 production in epidermal
663 keratinocytes. Sci Rep 6:31119.

664 Janke, M., J. Poth, V. Wimmenauer, T. Giese, C. Coch, W. Barchet, M. Schlee, and G. Hartmann. 2009.
665 Selective and direct activation of human neutrophils but not eosinophils by Toll-like receptor 8. The
666 Journal of allergy and clinical immunology 123:1026-1033.

667 Jurk, M., A. Kritzler, B. Schulte, S. Tluk, C. Schetter, A.M. Krieg, and J. Vollmer. 2006. Modulating
668 responsiveness of human TLR7 and 8 to small molecule ligands with T-rich phosphorothiate
669 oligodeoxynucleotides. European Journal of Immunology 36:1815-1826.

670 Kawasaki, T., and T. Kawai. 2014. Toll-like receptor signaling pathways. Front Immunol 5:461.

671 Kruger, P., M. Saffarzadeh, A.N. Weber, N. Rieber, M. Radsak, H. von Bernuth, C. Benarafa, D. Roos, J.
672 Skokowa, and D. Hartl. 2015. Neutrophils: Between host defence, immune modulation, and tissue
673 injury. PLoS Pathog 11:e1004651.

674 Kuznik, A., M. Bencina, U. Svajger, M. Jeras, B. Rozman, and R. Jerala. 2011. Mechanism of
675 endosomal TLR inhibition by antimalarial drugs and imidazoquinolines. Journal of Immunology
676 186:4794-4804.

677 Lande, R., E. Botti, C. Jandus, D. Dojcinovic, G. Fanelli, C. Conrad, G. Chamilos, L. Feldmeyer, B.
678 Marinari, S. Chon, L. Vence, V. Riccieri, P. Guillaume, A.A. Navarini, P. Romero, A. Costanzo, E.
679 Piccolella, M. Gilliet, and L. Frasca. 2014. The antimicrobial peptide LL37 is a T-cell autoantigen in
680 psoriasis. Nat Commun 5:5621.

681 Lande, R., D. Ganguly, V. Facchinetti, L. Frasca, C. Conrad, J. Gregorio, S. Meller, G. Chamilos, R.
682 Sebasigari, V. Riccieri, R. Bassett, H. Amuro, S. Fukuhara, T. Ito, Y.J. Liu, and M. Gilliet. 2011.
683 Neutrophils activate plasmacytoid dendritic cells by releasing self-DNA-peptide complexes in
684 systemic lupus erythematosus. Sci Transl Med 3:73ra19.

685 Lande, R., J. Gregorio, V. Facchinetti, B. Chatterjee, Y.H. Wang, B. Homey, W. Cao, B. Su, F.O. Nestle,
686 T. Zal, I. Mellman, J.M. Schroder, Y.J. Liu, and M. Gilliet. 2007. Plasmacytoid dendritic cells sense self-
687 DNA coupled with antimicrobial peptide. Nature 449:564-569.

688 Li, Q., Y. Kim, J. Namm, A. Kulkarni, G.R. Rosania, Y.H. Ahn, and Y.T. Chang. 2006. RNA-selective, live
689 cell imaging probes for studying nuclear structure and function. Chem Biol 13:615-623.

690 Li, X.D., and Z.J. Chen. 2012. Sequence specific detection of bacterial 23S ribosomal RNA by TLR13.
691 Elife 1:e00102.

692 Lindau, D., J. Mussard, B.J. Wagner, M. Ribon, V.M. Ronnefarth, M. Quettier, I. Jelcic, M.C. Boissier,
693 H.G. Rammensee, and P. Decker. 2013. Primary blood neutrophils express a functional cell surface
694 Toll-like receptor 9. European Journal of Immunology 43:2101-2113.

695 Matsukura, S., F. Kokubu, M. Kurokawa, M. Kawaguchi, K. Ieki, H. Kuga, M. Odaka, S. Suzuki, S.
696 Watanabe, T. Homma, H. Takeuchi, K. Nohtomi, and M. Adachi. 2007. Role of RIG-I, MDA-5, and PKR
697 on the expression of inflammatory chemokines induced by synthetic dsRNA in airway epithelial cells.
698 Int Arch Allergy Immunol 143 Suppl 1:80-83.

699 Menten, P., A. Wuyts, and J. Van Damme. 2002. Macrophage inflammatory protein-1. Cytokine
700 Growth Factor Rev 13:455-481.

701 Morizane, S., and R.L. Gallo. 2012. Antimicrobial peptides in the pathogenesis of psoriasis. J Dermatol
702 39:225-230.

703 Morizane, S., K. Yamasaki, B. Muhleisen, P.F. Kotol, M. Murakami, Y. Aoyama, K. Iwatsuki, T. Hata,
704 and R.L. Gallo. 2012. Cathelicidin antimicrobial peptide LL-37 in psoriasis enables keratinocyte
705 reactivity against TLR9 ligands. The Journal of investigative dermatology 132:135-143.

706 Neumann, A., E.T. Berends, A. Nerlich, E.M. Molhoek, R.L. Gallo, T. Meerloo, V. Nizet, H.Y. Naim, and
707 M. von Kockritz-Blickwede. 2014. The antimicrobial peptide LL-37 facilitates the formation of
708 neutrophil extracellular traps. Biochem J 464:3-11.

709 Noll, F., J. Behnke, S. Leiting, K. Troidl, G.T. Alves, H. Muller-Redetzky, K.T. Preissner, and S. Fischer.
710 2017. Self-extracellular RNA acts in synergy with exogenous danger signals to promote inflammation.
711 PLoS One 12:e0190002.

712 Radic, M., and T.N. Marion. 2013. Neutrophil extracellular chromatin traps connect innate immune
713 response to autoimmunity. Seminars in immunopathology 35:465-480.

714 Roth, S., W. Solbach, and T. Laskay. 2016. IL-16 and MIF: messengers beyond neutrophil cell death.
715 Cell Death Dis 7:e2049.

716 Saitoh, T., J. Komano, Y. Saitoh, T. Misawa, M. Takahama, T. Kozaki, T. Uehata, H. Iwasaki, H. Omori,
717 S. Yamaoka, N. Yamamoto, and S. Akira. 2012. Neutrophil extracellular traps mediate a host defense
718 response to human immunodeficiency virus-1. Cell Host Microbe 12:109-116.

719 Schauber, J., R.A. Dorschner, A.B. Coda, A.S. Buchau, P.T. Liu, D. Kiken, Y.R. Helfrich, S. Kang, H.Z.
720 Elalieh, A. Steinmeyer, U. Zugel, D.D. Bikle, R.L. Modlin, and R.L. Gallo. 2007. Injury enhances TLR2
721 function and antimicrobial peptide expression through a vitamin D-dependent mechanism. The
722 Journal of clinical investigation 117:803-811.

723 Schmidt, N.W., F. Jin, R. Lande, T. Curk, W. Xian, C. Lee, L. Frasca, D. Frenkel, J. Dobnikar, M. Gilliet,
724 and G.C. Wong. 2015. Liquid-crystalline ordering of antimicrobial peptide-DNA complexes controls
725 TLR9 activation. Nat Mater 14:696-700.

726 Schon, M.P., S.M. Broekaert, and L. Erpenbeck. 2017. Sexy again: the renaissance of neutrophils in
727 psoriasis. Exp Dermatol 26:305-311.

728 Sen, B.B., E.N. Rifaioglu, O. Ekiz, M.U. Inan, T. Sen, and N. Sen. 2013. Neutrophil to lymphocyte ratio
729 as a measure of systemic inflammation in psoriasis. Cutan Ocul Toxicol

730 Sorensen, O., K. Arnljots, J.B. Cowland, D.F. Bainton, and N. Borregaard. 1997. The human
731 antibacterial cathelicidin, hCAP-18, is synthesized in myelocytes and metamyelocytes and localized to
732 specific granules in neutrophils. Blood 90:2796-2803.

733 Tabeta, K., K. Hoebe, E.M. Janssen, X. Du, P. Georgel, K. Crozat, S. Mudd, N. Mann, S. Sovath, J.
734 Goode, L. Shamel, A.A. Herskovits, D.A. Portnoy, M. Cooke, L.M. Tarantino, T. Wiltshire, B.E.
735 Steinberg, S. Grinstein, and B. Beutler. 2006. The Unc93b1 mutation 3d disrupts exogenous antigen
736 presentation and signaling via Toll-like receptors 3, 7 and 9. Nature Immunology 7:156-164.

737 Tecchio, C., A. Micheletti, and M.A. Cassatella. 2014. Neutrophil-derived cytokines: facts beyond
738 expression. Front Immunol 5:508.

739 Terui, T., M. Ozawa, and H. Tagami. 2000. Role of neutrophils in induction of acute inflammation in T-
740 cell-mediated immune dermatosis, psoriasis: a neutrophil-associated inflammation-boosting loop.
741 Experimental dermatology 9:1-10.

742 Vierbuchen, T., C. Bang, H. Rosigkeit, R.A. Schmitz, and H. Heine. 2017. The Human-Associated
743 Archaeon Methanosphaera stadtmanae Is Recognized through Its RNA and Induces TLR8-Dependent
744 NLRP3 Inflammasome Activation. Front Immunol 8:1535.

745 Warnatsch, A., M. Ioannou, Q. Wang, and V. Papayannopoulos. 2015. Inflammation. Neutrophil
746 extracellular traps license macrophages for cytokine production in atherosclerosis. Science 349:316-
747 320.

748 Yao, Y., L. Richman, C. Morehouse, M. de los Reyes, B.W. Higgs, A. Boutrin, B. White, A. Coyle, J.
749 Krueger, P.A. Kiener, and B. Jallal. 2008. Type I interferon: potential therapeutic target for psoriasis?
750 PLoS One 3:e2737.

751 Yasuda, K., P. Yu, C.J. Kirschning, B. Schlatter, F. Schmitz, A. Heit, S. Bauer, H. Hochrein, and H.
752 Wagner. 2005. Endosomal translocation of vertebrate DNA activates dendritic cells via TLR9-
753 dependent and -independent pathways. J Immunol 174:6129-6136.

754 Zhang, L.J., G.L. Sen, N.L. Ward, A. Johnston, K. Chun, Y. Chen, C. Adase, J.A. Sanford, N. Gao, M.
755 Chensee, E. Sato, Y. Fritz, J. Baliwag, M.R. Williams, T. Hata, and R.L. Gallo. 2016. Antimicrobial
756 Peptide LL37 and MAVS Signaling Drive Interferon-beta Production by Epidermal Keratinocytes
757 during Skin Injury. Immunity 45:119-130.

758

759 Abbreviations

760 APC – antigen-presenting cell; bRNA – bacterial ribonucleic acid; Enhanced green fluorescence
761 protein – EGFP; Human embryonic kidney – HEK; HLA – Human leucocyte antigen; iODN – inhibitory
762 oligonucleotides; Microbe-associated molecular pattern – MAMPs; MHC – Major histocompatibility
763 complex; Inhibitory oligodeoxynucleotides – iODNs; Interferon – IFN; Interleukin – IL; Keratinocytes –
764 KC; PASI – psoriasis area and severity; Plasmacytoid dendritic cells – pDCs; PMA – phorbol myristate

765 acetate; Pattern recognition receptor – PRR; Polymorphonuclear leukocytes – PMNs; NE - Neutrophil
766 elastase; Neutrophil extracellular trap - NET; Scanning electron microscopy – SEM; Systemic lupus
767 erythematosus – SLE; TLR – Toll-like receptor; Tumor necrosis factor (TNF).

768 ## Figure legends

769 **Figure 1: Human neutrophils take up and respond to RNA when complexed to LL37**
770 (A-C) IL-8 release (ELISA, 4 h stimulation) and CD62L shedding (flow cytometry, 1 or 2 h) by PMNs
771 from healthy donors stimulated with LPS, R848 or CpG ODN (A, n=6-7), ssDNA and genomic DNA (B,
772 n=5), or RNA40 (C, n=8-15), with or without LL37. (D) Electron microscopy of PMNs incubated with
773 RNA-LL37 for 20 min (n=1). (E-H) FACS (E, n=6), ImageStream cytometry (F, G, scale bar = 10 µm) or
774 conventional bright-field microscopy (H, n=2, scale bar = 10 µm) of PMNs incubated for 60 min with
775 RNA-AF647 complexed with LL37 (n=6). In F the % of cells with 'internalized' features are shown
776 (n=2, see Methods), in G selected cells from one representative donor are shown. In H unmodified
777 LL37 was replaced with Atto488-labeled LL37, one representative donor shown. (I) as in C but
778 including chloroquine (CQ) pre-incubation for 30 min (n=6-7). PMN activation by human mRNA (J,
779 hRNA, n=4-6) and bacterial RNA (K, bRNA from *S. aureus,* n=4) with and without LL37. A-C, E, F, I-K
780 represent combined data (mean+SD) from 'n' biological replicates (each dot represents one donor).
781 In D, G and H one representative of 'n' biological replicates (donors) is shown (mean+SD). * $p<0.05$
782 according to one-way ANOVA with Dunnett's correction (A, B, C, I, J) or Friedman test with Dunn's
783 correction (E, K).

784 **Figure 2: RNA-LL37 complexes promote release of multiple pro-inflammatory cytokines and**
785 **chemokines, especially in psoriasis PMN**
786 Cytometric bead array (A-C) or ELISA (D, E) for TNF (A), IL-6 (B), IL-1β (C), IL-16 (D) or MIP-1β (E)
787 secreted from PMNs stimulated for 4 h as indicated (n=6). Flow cytometric cell counts of migrated
788 CD4 T cells (F, I), CD8 T cells (G) and $CD14^{+}HLA\text{-}DR^{+}$ monocytes (H) quantified in transwell assays with
789 total PBMCs in the upper and either MIP-1β (30 and 150 pg/ml) or IL-16 (300 and 1500 pg/ml) (F-H,
790 n=6-7, $p>0.05$ for treatments vs. media) or R848, RNA with and without LL37 (I, n=3-7) in the lower
791 chamber. (J, K) ELISA of IL-8 and MIP-1β secreted from psoriasis PMNs (n=3 patients, , squares,
792 chequered bars) or PMNs from sex-and age-matched healthy donors (n=10, circles, filled bars). (L) as
793 in J or K but ELISA for LL37 (n=4 patients, 7 healthy donors). A-K represent combined data (mean+SD)
794 from 'n' biological replicates (each dot represents one donor). * $p<0.05$ according to Friedmann test
795 with Dunn's correction (A, B, D-H), or one-way ANOVA with Dunnett's correction for multiple testing
796 (C, I, J-L).

797 **Figure 3: RNA-LL37 trigger the release of NETs containing further RNA, DNA and LL37**
798 (A) EM pictures from PMNs stimulated with RNA-LL37 (n=2). (B) Neutrophil elastase (NE) release
799 from PMNs stimulated for 3 h (n=8, each dot representing one donor). Fluorescence microscopy of
800 fixed and Hoechst, anti-LL37, SYTO RNAselect- (C) and/or anti-ΨU-stained (D, with or without RNase

801 A treatment) or live (E) PMNs stimulated as indicated (n=6, scale bar = 10 µm or n=4, scale bar = 20
802 µm). (F) Quantification of live cell microscopy), see also Movies S1-S3. (G, H) Skin sections from
803 healthy (G) or psoriasis- (G, H) affected skin (n=12 patients and 3 healthy controls, scale bar = 20 µm).
804 (I, J) as in C (left panels) and stimulated with transferred NETs (right panels). AF = autofluorescence.
805 B, F and I represent combined data (mean+SD) from 'n' biological replicates. In A, C-E, H and J
806 representative samples of 'n' replicates or donors are shown. Arrowheads indicate released
807 RNA/NETs (C-E) or RNA-LL37 co-localization (H). * $p<0.05$ according to one-way ANOVA (B), two-way
808 ANOVA (F) with Dunnett's correction or Kruskal-Wallis test with Dunn's correction (I).

809 **Figure 4: RNA-LL37 effects in primary PMNs are mediated by TLR8/TLR13 and can be inhibited by**
810 **Inhibitory oligodeoxynucleotides**

811 (A) Tnf release (ELISA, 5 h stimulation as indicated) by BM-PMNs from different mouse strains (n=4-8
812 each). (B, C) Fluorescence microscopy of fixed, Hoechst and SYTO RNAselect-stained stimulated BM-
813 PMNs (n=4 *Tlr13*$^{-/-}$, n=5 *Unc93b1*$^{3d/3d}$, n=8 WT, scale bar = 10 or 20 µm, respectively). (D) Relative IL-
814 8release (ELISA, 18 h stimulation as indicated) by WT and *TLR8* CRISPR-edited BlaER1 cells,
815 normalized to *E. coli* control (n=4). (E) NF-κB dual luciferase reporter assay in HEK293T cells,
816 transfected with NF-κB firefly luciferase reporter, *Renilla* control reporter, TLR8 plasmid or empty
817 vector (EV), and subsequently stimulated with RNA without (arrow) or with IRS661, IRS954, IRS869
818 and IRS546 (0.15-3.5 µM, n=2 each). IL-8 (F, n=6) or MIP-1β (G, n=4) release from stimulated PMNs
819 with or without IRS661 (1 nM) or IRS954 (50 nM) pre-incubation (30 min) quantified by ELISA. (H)
820 Fluorescence microscopy of fixed Hoechst and anti-ΨU-stained RNA-LL37-stimulated PMNs (n=3,
821 scale bar = 10 µm). (I) Quantification of H. A, D- G and I represent combined data (mean+SD) from 'n'
822 biological replicates (each dot represents one mouse, donor or measurement). In B, C, E and H one
823 representative of 'n' replicates is shown (mean+SD of technical triplicates). * $p<0.05$ according to
824 two-way ANOVA with Dunnett correction for multiple testing (E, comparison against 'no inhibitor'
825 condition, arrow), one-way ANOVA with Sidak correction (A, D, F), Friedmann test with Dunn
826 correction (G) or Mann-Whitney test (I).

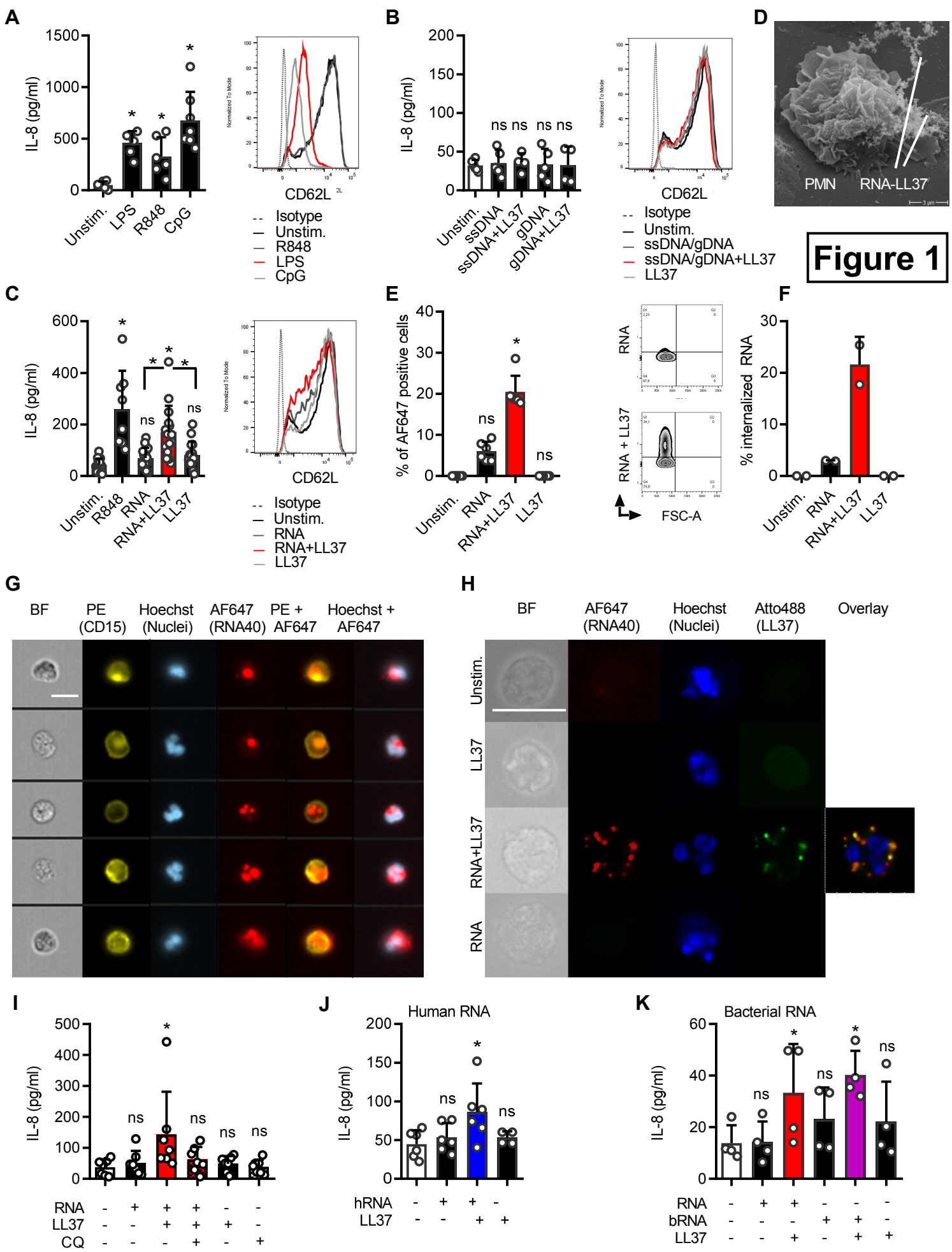
A
IL-8 (pg/ml)
Unstim.
LPS
R848
CpG
CD62L
Isotype
Unstim.
R848
LPS
CpG
B
IL-8 (pg/ml)
ns ns ns ns
Unstim.
ssDNA
ssDNA+LL37
gDNA
gDNA+LL37
CD62L
Isotype
Unstim.
ssDNA/gDNA
ssDNA/gDNA+LL37
LL37
D
PMN
RNA-LL37
Figure 1
C
IL-8 (pg/ml)
ns
Unstim.
R848
RNA
RNA+LL37
LL37
CD62L
Isotype
Unstim.
RNA
RNA+LL37
LL37
E
% of AF647 positive cells
ns
Unstim.
RNA
RNA+LL37
LL37
RNA
RNA + LL37
FSC-A
F
% internalized RNA
Unstim.
RNA
RNA+LL37
LL37
G
BF
PE (CD15)
Hoechst (Nuclei)
AF647 (RNA40)
PE + AF647
Hoechst + AF647
H
BF
AF647 (RNA40)
Hoechst (Nuclei)
Atto488 (LL37)
Overlay
Unstim.
LL37
RNA+LL37
RNA
I
IL-8 (pg/ml)
ns
RNA
LL37
CQ
J
Human RNA
IL-8 (pg/ml)
ns
hRNA
LL37
K
Bacterial RNA
IL-8 (pg/ml)
ns
RNA
bRNA
LL37

Figure 2

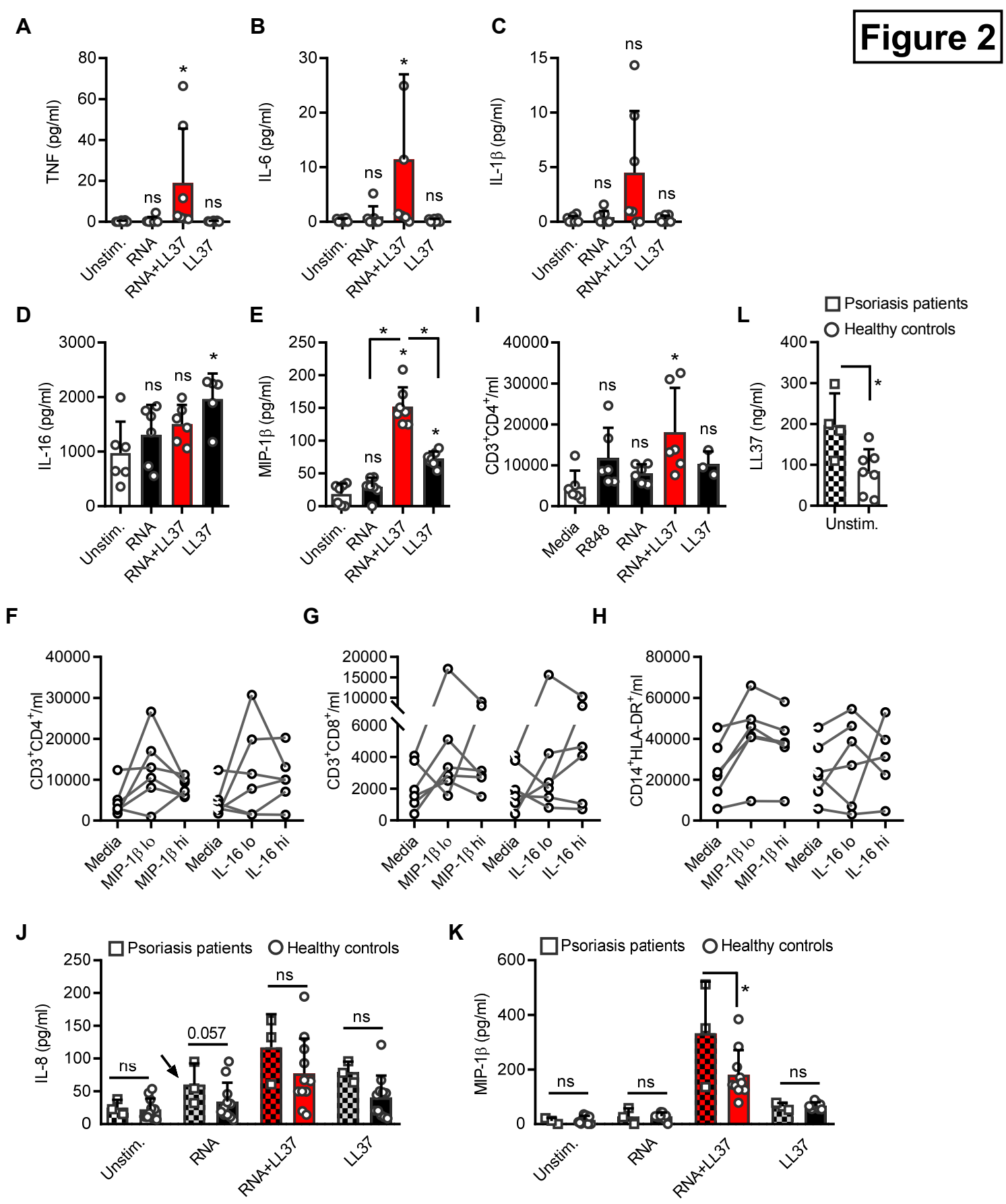
A
TNF (pg/ml)
80
60
40
20
0
ns
*
ns
Unstim.
RNA
RNA+LL37
LL37
B
IL-6 (pg/ml)
30
20
10
0
ns
*
ns
Unstim.
RNA
RNA+LL37
LL37
C
IL-1β (pg/ml)
15
10
5
0
ns
ns
ns
Unstim.
RNA
RNA+LL37
LL37
D
IL-16 (pg/ml)
3000
2000
1000
0
ns
ns
*
Unstim.
RNA
RNA+LL37
LL37
E
MIP-1β (pg/ml)
250
200
150
100
50
0
*
*
*
ns
*
Unstim.
RNA
RNA+LL37
LL37
I
CD3+CD4+/ml
40000
30000
20000
10000
0
ns
*
ns
ns
Media
R848
RNA
RNA+LL37
LL37
L
Psoriasis patients
Healthy controls
LL37 (ng/ml)
400
300
200
100
0
*
Unstim.
F
CD3+CD4+/ml
40000
30000
20000
10000
0
Media
MIP-1β lo
MIP-1β hi
Media
IL-16 lo
IL-16 hi
G
CD3+CD8+/ml
20000
15000
10000
6000
4000
2000
0
Media
MIP-1β lo
MIP-1β hi
Media
IL-16 lo
IL-16 hi
H
CD14+HLA-DR+/ml
80000
60000
40000
20000
0
Media
MIP-1β lo
MIP-1β hi
Media
IL-16 lo
IL-16 hi
J
Psoriasis patients
Healthy controls
IL-8 (pg/ml)
250
200
150
100
50
0
ns
0.057
ns
ns
Unstim.
RNA
RNA+LL37
LL37
K
Psoriasis patients
Healthy controls
MIP-1β (pg/ml)
600
400
200
0
ns
ns
*
ns
Unstim.
RNA
RNA+LL37
LL37

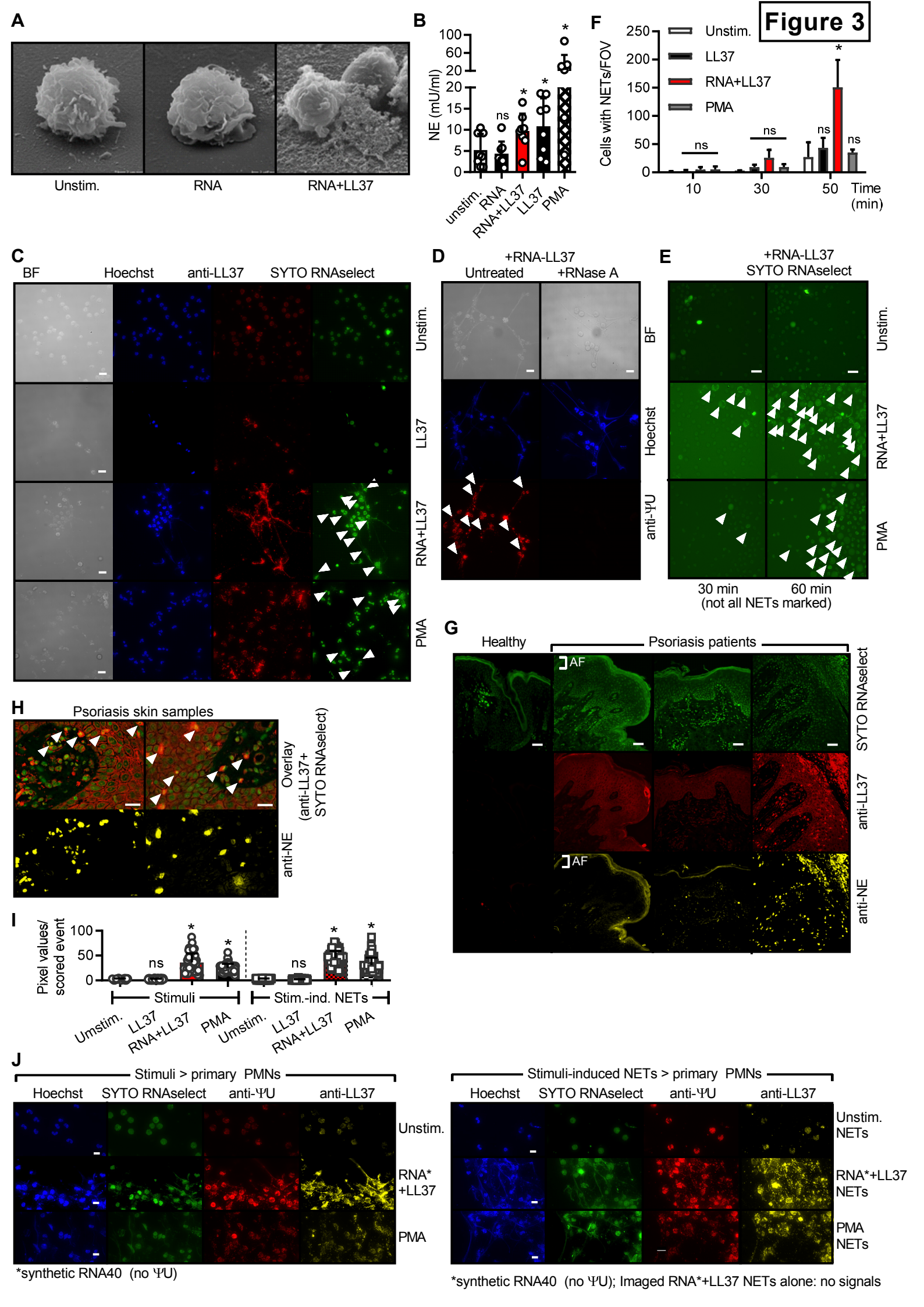
Figure 3
A
Unstim.
RNA
RNA+LL37
B
NE (mU/ml)
100
60
20
20
15
10
5
0
ns
*
*
*
unstim.
RNA
RNA+LL37
LL37
PMA
F
Cells with NETs/FOV
250
200
150
100
50
0
Unstim.
LL37
RNA+LL37
PMA
ns
ns
ns
ns
*
10
30
50
Time (min)
C
BF
Hoechst
anti-LL37
SYTO RNAselect
Unstim.
LL37
RNA+LL37
PMA
D
+RNA-LL37
Untreated
+RNase A
BF
Hoechst
anti-ΨU
E
+RNA-LL37
SYTO RNAselect
Unstim.
RNA+LL37
PMA
30 min
60 min
(not all NETs marked)
G
Healthy
Psoriasis patients
AF
AF
SYTO RNAselect
anti-LL37
anti-NE
H
Psoriasis skin samples
Overlay (anti-LL37+ SYTO RNAselect)
anti-NE
I
Pixel values/ scored event
100
50
0
ns
ns
*
*
*
*
Stimuli
Stim.-ind. NETs
Unstim.
LL37
RNA+LL37
PMA
Unstim.
LL37
RNA+LL37
PMA
J
Stimuli > primary PMNs
Hoechst
SYTO RNAselect
anti-ΨU
anti-LL37
Unstim.
RNA* +LL37
PMA
*synthetic RNA40 (no ΨU)
Stimuli-induced NETs > primary PMNs
Hoechst
SYTO RNAselect
anti-ΨU
anti-LL37
Unstim. NETs
RNA*+LL37 NETs
PMA NETs
synthetic RNA40 (no ΨU); Imaged RNA+LL37 NETs alone: no signals

Figure 4

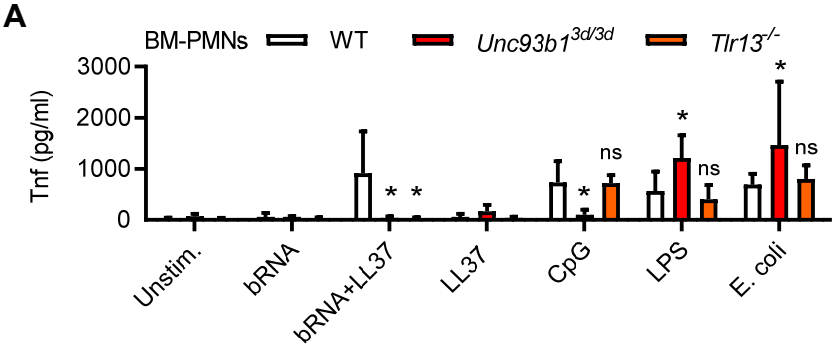
A
BM-PMNs
WT
Unc93b1 3d/3d
Tlr13 -/-
Tnf (pg/ml)
3000
2000
1000
0
Unstim.
bRNA
bRNA+LL37
LL37
CpG
LPS
E. coli
ns

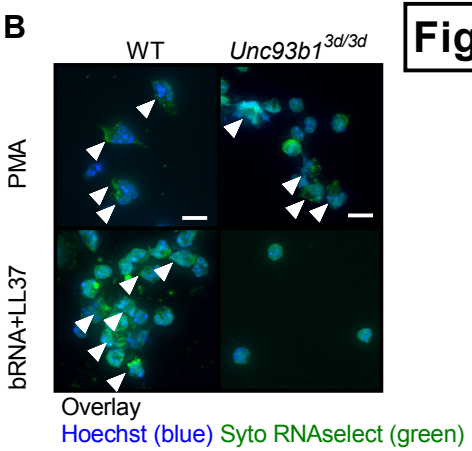
B
WT
Unc93b1 3d/3d
PMA
bRNA+LL37
Overlay
Hoechst (blue) Syto RNAselect (green)

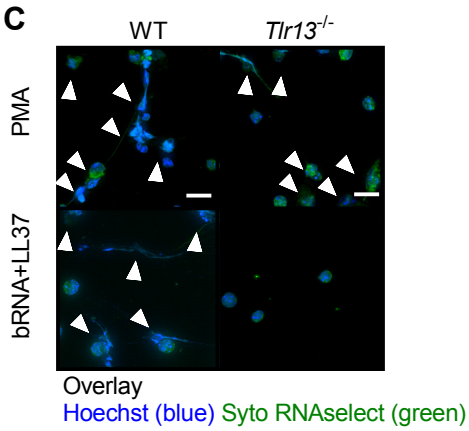
C
WT
Tlr13 -/-
PMA
bRNA+LL37
Overlay
Hoechst (blue) Syto RNAselect (green)

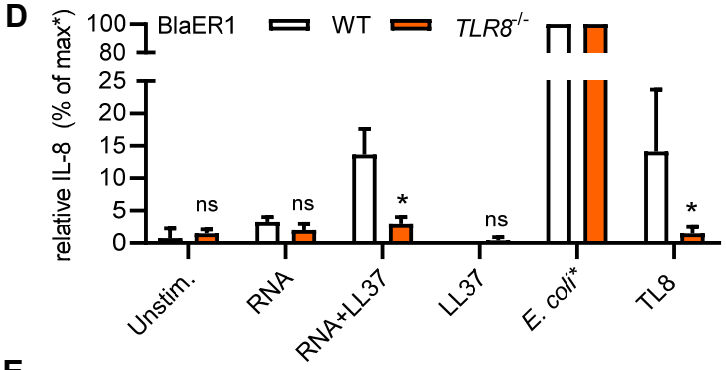
D
BlaER1
WT
TLR8 -/-
relative IL-8 (% of max*)
100
80
25
20
15
10
5
0
ns
Unstim.
RNA
RNA+LL37
LL37
E. coli*
TL8

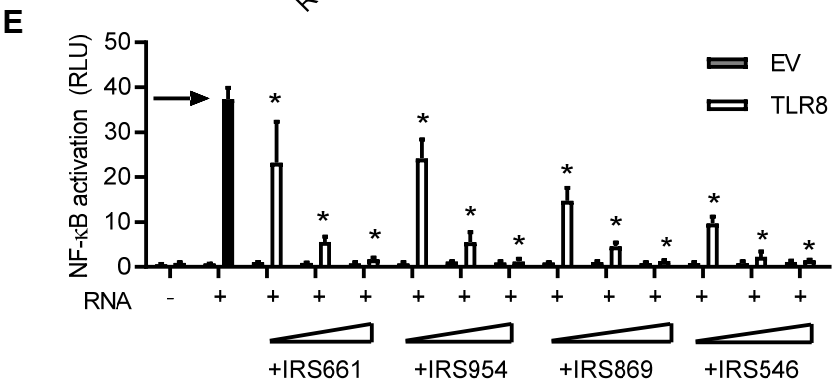
E
NF-κB activation (RLU)
50
40
30
20
10
0
EV
TLR8
RNA
+IRS661
+IRS954
+IRS869
+IRS546

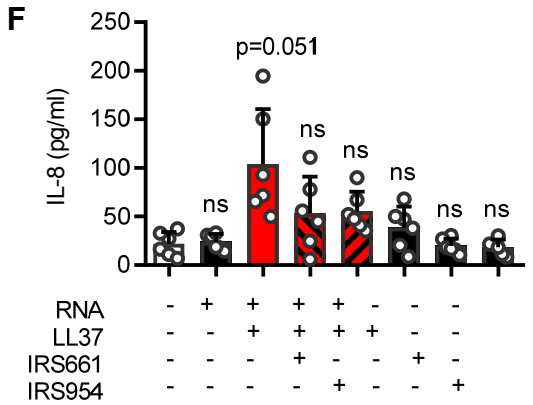
F
IL-8 (pg/ml)
250
200
150
100
50
0
p=0.051
ns
RNA
LL37
IRS661
IRS954

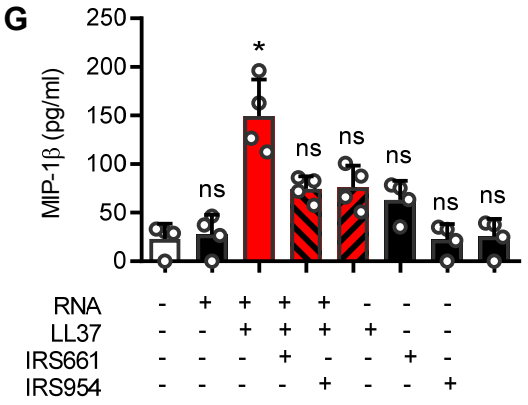
G
MIP-1β (pg/ml)
250
200
150
100
50
0
ns
RNA
LL37
IRS661
IRS954

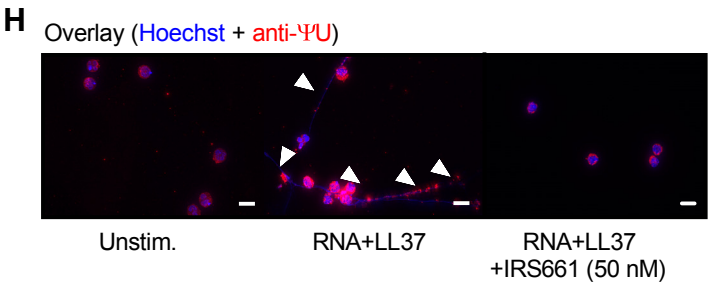
H
Overlay (Hoechst + anti-ΨU)
Unstim.
RNA+LL37
RNA+LL37
+IRS661 (50 nM)

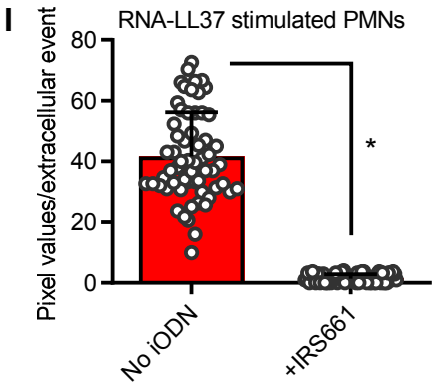
I
RNA-LL37 stimulated PMNs
Pixel values/extracellular event
80
60
40
20
0
No iODN
+IRS661